

Morphology-dependent pH-responsive release of hydrophilic payloads  
using biodegradable nanocarriers

Supplementary material

PRAMANIK, Sumit; SENECA, Senne; PETERS, Martijn; D'OLIESLAEGER, Lien;  
REEKMANS, Gunter; VANDERZANDE, Dirk; ADRIAENSENS, Peter & ETHIRAJAN,  
Anitha (2018) Morphology-dependent pH-responsive release of hydrophilic payloads  
using biodegradable nanocarriers. In: RSC Advances, 8(64), p. 36869-36878.

DOI: 10.1039/c8ra07066k

Handle: <http://hdl.handle.net/1942/27506>

## Electronic Supplementary Information

### **Morphology-dependent pH-responsive release of hydrophilic payloads using biodegradable nanocarriers**

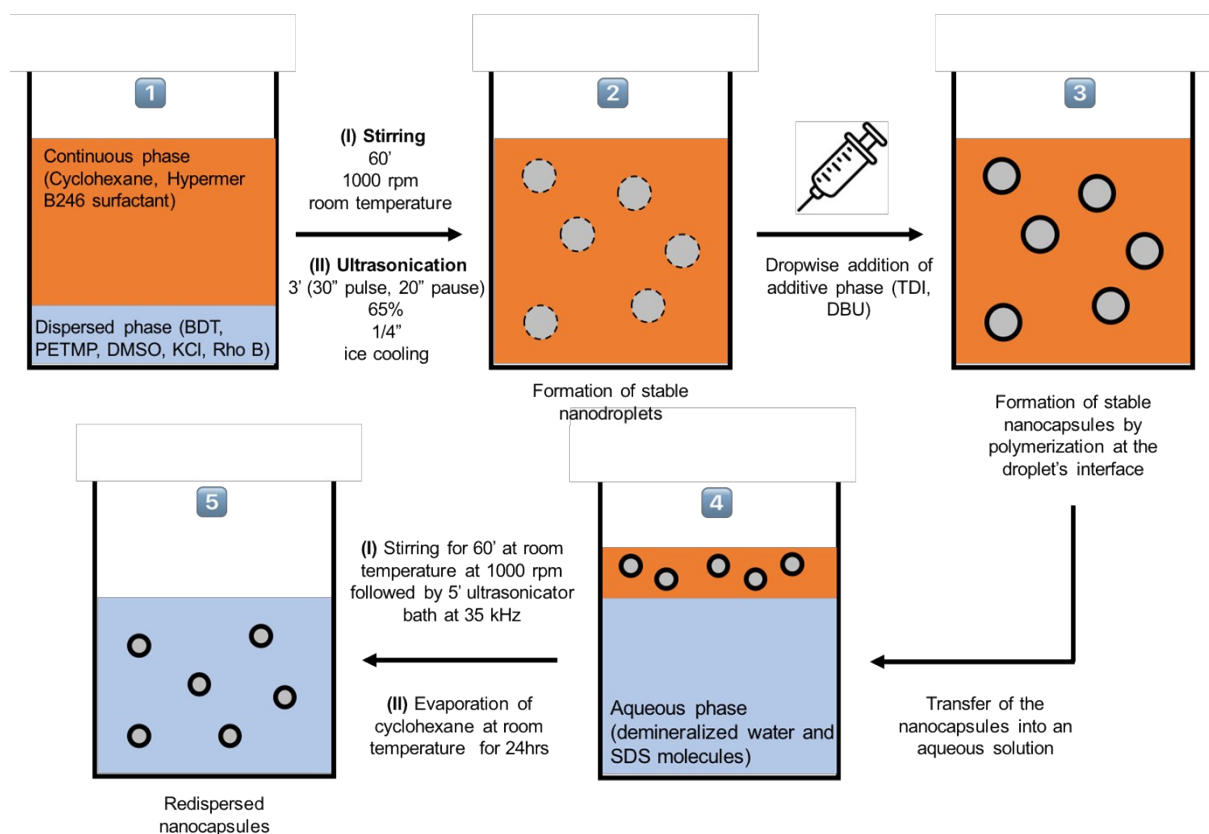
*Sumit Kumar Pramanik,<sup>a,b,≠</sup> Senne Seneca,<sup>a,b,≠</sup> Martijn Peters,<sup>a,b</sup> Lien D'Olieslaeger,<sup>a,b</sup> Gunter Reekmans,<sup>a,b</sup> Dirk Vanderzande,<sup>a,b</sup> Peter Adriaensens,<sup>a,b</sup> and Anitha Ethirajan<sup>\*a,b</sup>*

<sup>a</sup> Institute for Materials Research (IMO), Hasselt University, Wetenschapspark 1 and Agoralaan D, 3590 Diepenbeek, Belgium

<sup>b</sup> IMEC, associated lab IMOMECE, Wetenschapspark 1, 3590 Diepenbeek, Belgium

<sup>≠</sup> Both authors contributed equally.

Email: [anitha.ethirajan@uhasselt.be](mailto:anitha.ethirajan@uhasselt.be)



**Scheme S1.** A simplified schematic representation of the formulation process of pH-responsive polymeric poly(thiourethane-urethane) nanocarriers with ester linkages through a polyaddition reaction at the droplet interface using the inverse miniemulsion process, and the subsequent redispersion of nanocarriers in an aqueous phase for biomedical applications.

**Table S1. Characteristics of nanocarriers containing rhodamine B.**

<b>Sample</b>	<b>Dispersed Phase</b>	<b>Additive Phase</b>	<b>Size (nm) / PDI</b>		<b>Encapsulation Efficiency</b>
			<b>Cyclohexane</b>	<b>Aqueous</b>	
<b>1'</b>	4 mmol BDT, 0.2 mmol PETMP, 2 mg rhodamine B	4.2 mmol TDI, DBU	191 / 0.05	285 / 0.17 (291 / 0.21) <sup>a</sup> (285 / 0.17) <sup>b</sup> (287 / 0.23) <sup>c</sup>	88%
<b>2'</b>	3.6 mmol BDT, 0.4 mmol PCLD, 0.2 mmol PETMP, 2 mg rhodamine B	4.2 mmol TDI, DBU	194 / 0.10	283 / 0.18	91%
<b>3'</b>	3.2 mmol BDT, 0.8 mmol PCLD, 0.2 mmol PETMP, 2 mg rhodamine B	4.2 mmol TDI, DBU	217 / 0.09	281 / 0.14 (547 / 0.63) <sup>a</sup> (331 / 0.32) <sup>b</sup> (341 / 0.39) <sup>c</sup>	93%
<b>4'</b>	2.8 mmol BDT, 1.2 mmol PCLD, 0.2 mmol PETMP, 2 mg rhodamine B	4.2 mmol TDI, DBU	229 / 0.13	323 / 0.25	91%
<b>5'</b>	2 mmol BDT, 2 mmol PCLD, 0.2 mmol PETMP, 2 mg rhodamine B	4.2 mmol TDI, DBU	154 / 0.04	226 / 0.16	86%

<sup>a</sup> Size and PDI obtained after 8h at pH 4.0

<sup>b</sup> Size and PDI obtained after 8h at pH 6.5

<sup>c</sup> Size and PDI obtained after 8h at pH 9.0

**Table S2.** Summary of the encapsulation efficiency and loading content of rhodamine B dye for the synthesized samples.

<b>Sample</b>	<b>Encapsulation Efficiency</b>	<b>Experimental Loading Content</b>	<b>Theoretical Loading Content</b>
<b>1</b>	88%	0.081%	0.082%
<b>2</b>	91%	0.072%	0.076%
<b>3</b>	93%	0.068%	0.069%
<b>4</b>	91%	0.061%	0.065%
<b>5</b>	86%	0.050%	0.055%

**FT-IR analysis**

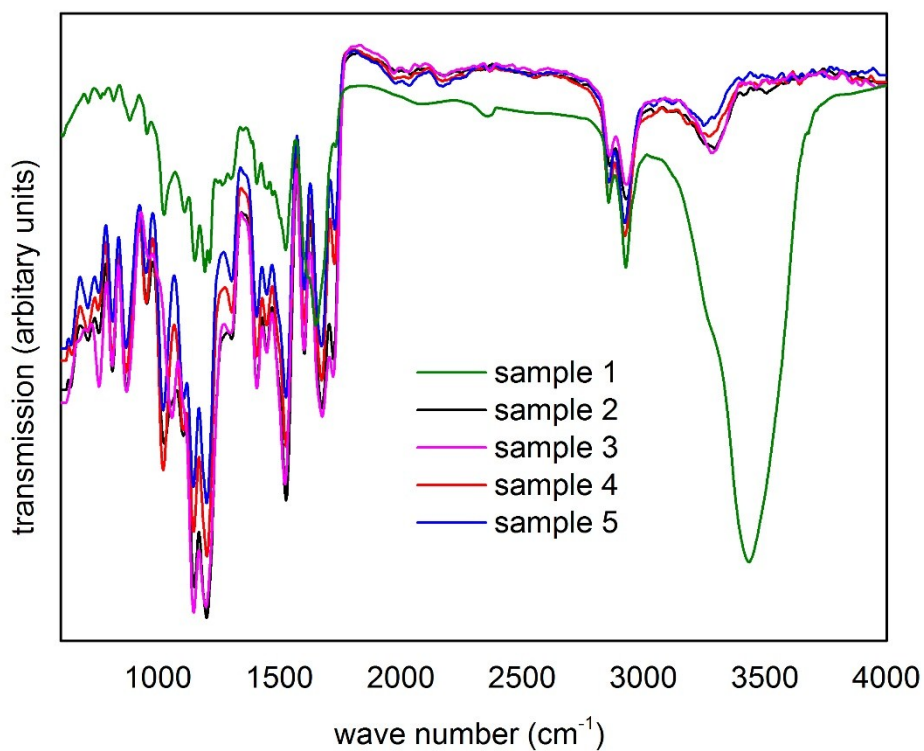


**Figure S1.** FT-IR spectra of all samples (sample 1-5).

Figure S1. All spectra clearly demonstrate a broad peak at 3300 cm<sup>-1</sup> due to O-H vibration originating from the surfactant and water, and characteristic C-H stretching vibration occurring at 2929 cm<sup>-1</sup> and 2849 cm<sup>-1</sup> as a result of CH<sub>2</sub> vibration.

### Size distribution of the nanocarriers

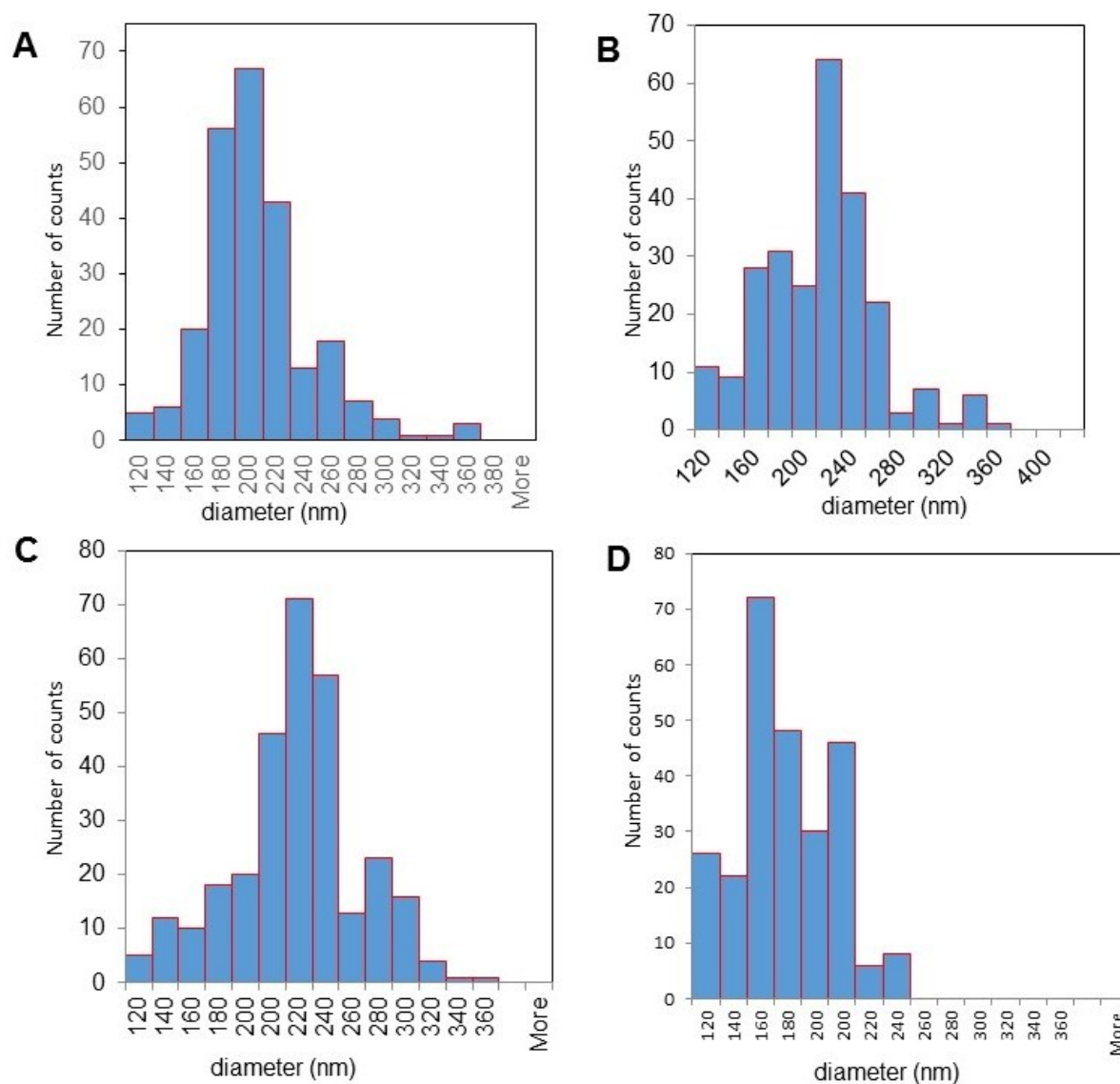


**Figure S2.** Size distribution of the nanocarriers obtained from TEM images for sample 2 (A), sample 3 (B), sample 4 (C) and sample 5 (D).

Figure S2. For sample 2-4, the size and size distribution broadens with increasing amounts of PCLD. For samples 2-4, the average size of the nanocapsules determined was respectively  $206 \pm 51$  nm,  $212 \pm 66$  nm and  $221 \pm 74$  nm. For sample 5, which demonstrated nanoparticle morphology, the size determined was  $173 \pm 41$  nm. Here, HClmage processing and image analysis tools have been used for quantitative analysis of more than 250 nanocapsules.

### **Alamar Blue assay**

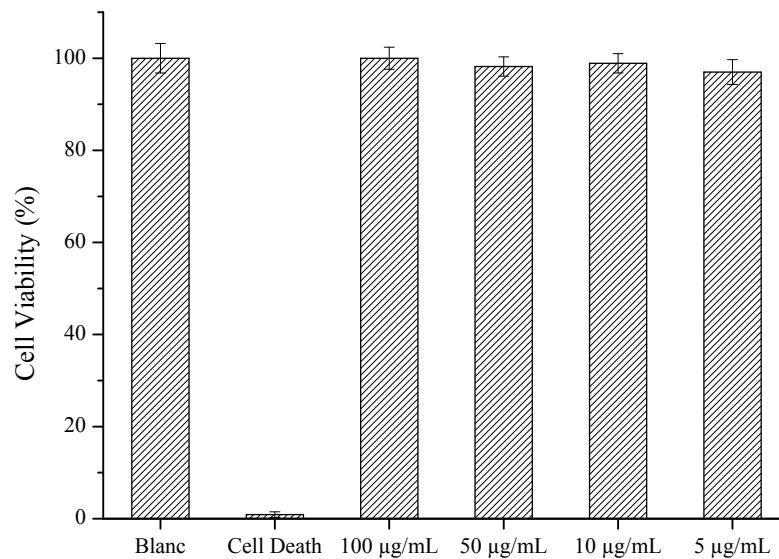


**Figure S3.** Cell viability of HeLa cells after 24h exposure to a concentration range of nanocarriers (sample 3), determined using the Alamar Blue assay. Data represent mean  $\pm$  standard deviation ( $N = 3$ ).

### **Cellular uptake of nanocarriers**

#### **Confocal Laser Scanning Microscopy Imaging**

HeLa cells were seeded on microscope glasses in a 24-well plate at 30 000 cells per well and left to incubate for 24 h at 37 °C in 5 % CO<sub>2</sub>. After washing the cells with 1xPBS, a 75 µg/mL solution of nanocarriers in supplemented IMDM culture medium was added to the cells and left to incubate for 6 h. After rinsing the cells with 1xPBS at 37 °C, 200 µL of fixation/extraction/permeabilization buffer (4 v/v % PFA supplemented with 0.3 v/v % triton x-100 and 5.0 w/v % sucrose) was added at RT on a shaker at 50 rpm for 2 h. Cells were washed 3 times with washing buffers (1xPBS containing 0.1 % triton x-100) after which 200 µL of blocking buffer (1xPBS containing 0.1 % triton x-100 and 2 % Bovine Serum Albumin) was added for 1 h at 50 rpm on a shaker at RT. Subsequently, the cells were incubated at RT with 200 µL of primary antibody (mouse monoclonal anti- $\alpha$ -tubulin, 1:1000 in blocking buffer) for 1h at 50 rpm and were then rinsed 3 times with washing buffer at 50 rpm for 5 min. Next, the cells were incubated for 1h at RT with 200 µL of secondary Ab (donkey anti-mouse



Alexa Fluor 488, 1:250 in blocking buffer) at 50 rpm. After washing with washing buffer for 5 min at 50 rpm, 200  $\mu$ L of DAPI (1:25 in blocking buffer) was added for 1h at RT. The cells were rinsed 3 times with washing buffer and covered with mounting medium in order to prevent dye photobleaching. The stained HeLa cells were visualized at RT with the Zeiss LSM510 META NLO mounted on an inverted laser scanning microscope (Zeiss Axiovert 200 M) and a 40x/1.1 water immersion objective. Excitation of the tubulin and nanoparticles was done with an Argon-ion laser at 488 and 543 nm respectively (3  $\mu$ W maximum radiant power in the sample). Excitation of DAPI was done at 730 nm ( $\sim$ 5 mW average radiant power at the sample position) using a femtosecond pulsed titanium-sapphire MaiTai DeepSee laser. Emission was detected using band-pass filters 565-615 (NPs), 500-550 nm (tubulin) and 390-465 nm (DAPI). The resulting 1024x1024 images with a pixel size of 0.06  $\mu$ m were recorded using a pixel dwell time of 375  $\mu$ s and a fixed pinhole size of 240  $\mu$ m (tubulin), 600  $\mu$ m (NPs) and 1000  $\mu$ m (DAPI). The acquired mages were processed using AIM 4.2 and ImageJ software.

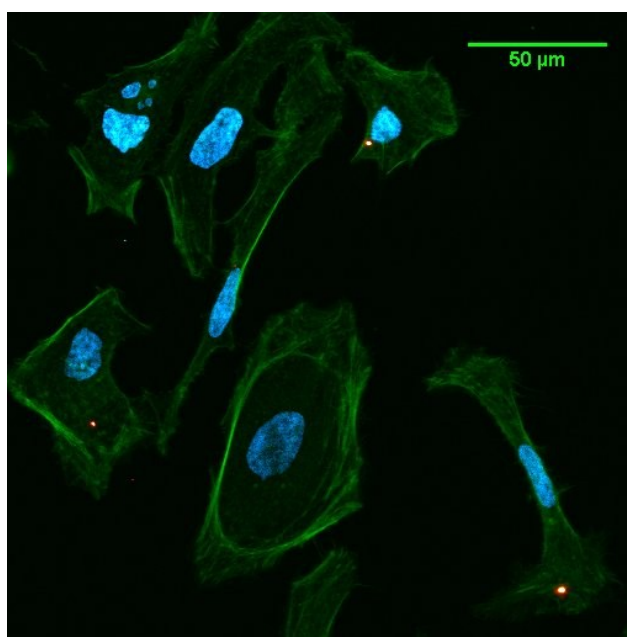


**Figure S4.** Fluorescence microscopy image of HeLa cells after 6h incubation with rhodamine B-loaded nanocapsules (orange) with additional staining of the cell nucleus (blue) and tubulin (green).